

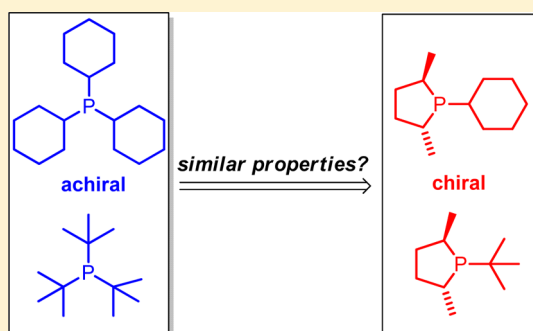
Chiral Monodentate Trialkylphosphines Based on the Phospholane Architecture

Pavel A. Donets, Tanguy Saget, and Nicolai Cramer*

Laboratory of Asymmetric Catalysis and Synthesis, Institute of Chemical Sciences and Engineering, Ecole Polytechnique Fédérale de Lausanne (EPFL), SB-ISIC, BCH4305, 1015 Lausanne, Switzerland

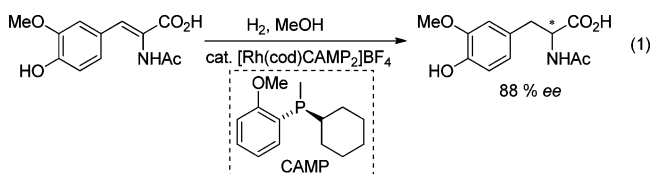
Supporting Information

ABSTRACT: The development of efficient chiral monodentate phosphine ligands lags behind that of the bidentate congeners. This holds especially true for highly electron rich chiral phosphine analogues able to replace the ubiquitous tricyclohexylphosphine and tri-*tert*-butylphosphine in catalytic asymmetric transformations. We present a convenient and modular synthesis of a set of chiral monodentate ligands with different steric demands based on the popular phospholane scaffold. Their steric and electronic properties were determined by their corresponding nickel and palladium complexes. They represent good mimics of the popular tricyclohexylphosphine and tri-*tert*-butylphosphine ligands. Their potential was subsequently evaluated in palladium-catalyzed asymmetric C(sp³)-H functionalization leading to indolines.



INTRODUCTION

Major breakthroughs in transition-metal catalysis have most often followed advances in ligand design. In particular, the developments of chiral, tailored phosphines as steering ligands is of utmost importance for asymmetric catalysis. Knowles, a pioneer in this field, reported asymmetric rhodium-catalyzed hydrogenation of dehydroamino acid derivatives en route to *L*-Dopa. One of the first successful chiral ligands, CAMP, which gave for that time a great enantioselectivity of 88% ee, was a monodentate phosphine (eq 1).¹ It was abandoned in favor of

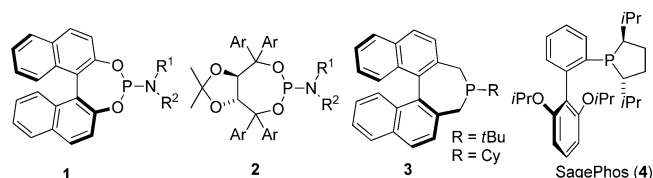


his famous DIPAMP, which was not only more easily accessible but gave a better enantioselectivity of 95% ee as well. The field of chiral bidentate phosphines has literally exploded in the following decades, and now, bidentate ligands are much more abundantly available than their monodentate counterparts. This imbalance holds true as well for the variability of their structural design.

However, over the past few years, an increasing number of catalytic transformations have been discovered which tolerate only a *single* ligand on the metal, leading to a renaissance of interest in monodentate phosphines as steering ligands. Despite their longstanding niche character, powerful and privileged scaffolds have been developed. For relatively electron poor phosphorus ligands, the phosphoramidite structures are clearly dominant. Two main classes, one derived from the binol

backbone (1)^{2,3} and one from the taddol backbone (2),⁴ largely dominate this field (Chart 1). They are easily accessible, and

Chart 1. Examples of Monodentate Chiral Phosphines



especially the taddol family exhibits a great modularity, a very attractive feature in adapting the ligand to the needs of the transformation. In contrast, more electron-rich phosphorus ligands, targeting complementary reactions, are less common,⁵ and in several instances chiral carbenes⁶ have replaced the phosphines.

Along our efforts to develop enantioselective C-H bond functionalizations,⁷ we required electron-rich monodentate phosphines. While the majority of the reported phosphines were not suitable, we reported a class of ligands, of which especially SagePhos (4; Chart 1) emerged as a very powerful ligand to induce excellent stereoselectivities in challenging palladium-catalyzed C(sp³)-H functionalizations.⁸ This structural scaffold can be seen as a chiral version of the Buchwald ligands.⁹ Similarly, there is as well a need for chiral versions of tricyclohexylphosphine and tri-*tert*-butylphosphine, the two electron-rich phosphines which are most ubiquitously utilized in catalysis. Those chiral versions should closely mimic the

Received: September 12, 2012

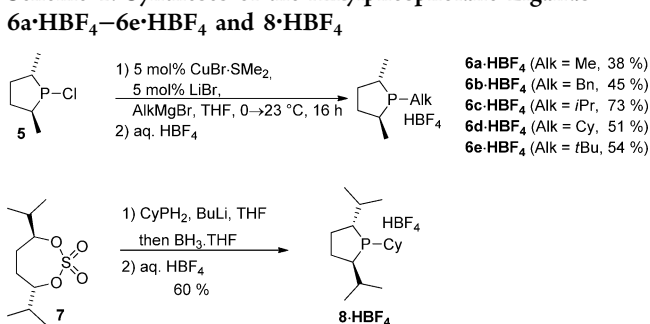
electronic and steric properties of the parent phosphines. In this respect, phosphine derivatives such as 3^{Sc-F} are currently the closest mimics. Surprisingly, trialkyl derivatives incorporating the good-performing, electron-rich, C_2 -symmetric phospholane scaffold¹⁰ have received only scarce attention so far.¹¹

RESULTS AND DISCUSSION

Synthesis of the Ligands and the Metal Complexes.

Chlorodimethylphospholane (**5**), which is accessible from the TMS-phospholane in one step,¹² was used as the key precursor. It was reacted in the presence of a catalytic amount of $CuBr \cdot SMe_2$ and lithium bromide with a range of alkyl Grignard reagents (Scheme 1). Using our previously reported extraction

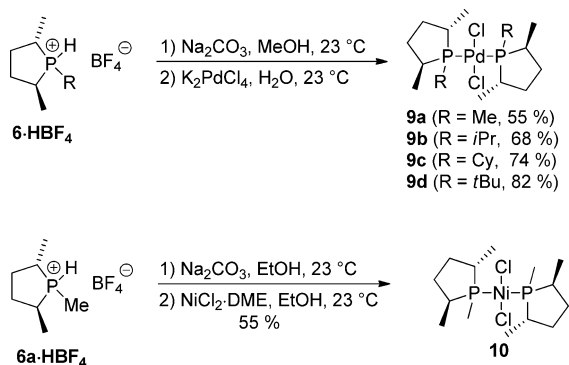
Scheme 1. Syntheses of the Alkylphospholane Ligands



protocol,¹³ the phosphines are conveniently isolated directly as their air-stable tetrafluoroborates **6a**·HBF₄–**6e**·HBF₄ and can be recrystallized subsequently. In general, this method provides the phosphonium salts in reasonable yields (38–73%) and high purities. For the synthesis of phospholane modules other than the 2,5-dimethyl derivatives, a route involving double alkylation¹⁴ and subsequent cleavage¹⁵ of the resulting phosphine–borane adduct was followed. For instance, preparation by double alkylation of the primary cyclohexylphosphine with the cyclic sulfate **7** provided the 2,5-diisopropyl derivative **8**·HBF₄ in 60% yield. With these two methods a variety of trialkylphosphines with different substitution patterns and gradually increasing steric demands were prepared.

We have next prepared palladium(II) and nickel(II) complexes of the phospholanes **6** (Scheme 2). The free phosphines were obtained by treatment with sodium carbonate in methanol and directly reacted with potassium tetrachloropalladate and nickel(II) chloride dimethoxyethane complex, respectively. After recrystallization from ethanol the palladium-

Scheme 2. Preparation of the Metal Complexes **9a–d** and **10**



(II) complexes **9a–d** and the nickel(II) complex **10** were obtained in 55–82% yield.¹⁶

As expected, the complexes **9b–d** showed the typical square-planar geometry for palladium(II) complexes with the phosphine ligands being trans to each other (Figures 1–3).

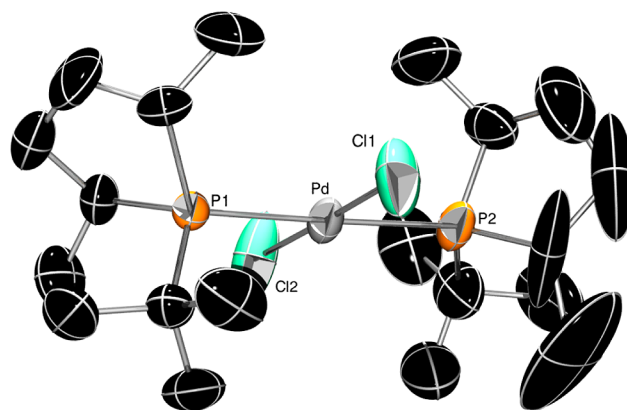


Figure 1. X-ray structure of complex **9d**. The thermal ellipsoids are displayed at 50% probability, and hydrogen atoms are omitted for clarity. Selected bond lengths (Å) and angles (deg): P1–Pd, 2.3547(13); P2–Pd, 2.3864(15); Cl1–Pd, 2.291(2); Cl2–Pd, 2.297(2); P1–Pd–P2, 178.53(6); Cl1–Pd–Cl2, 178.00(8); P1–Pd–Cl1, 89.92(6); P1–Pd–Cl2, 88.09(6); P2–Pd–Cl1, 89.14(7); P2–Pd–Cl2, 92.85(7).

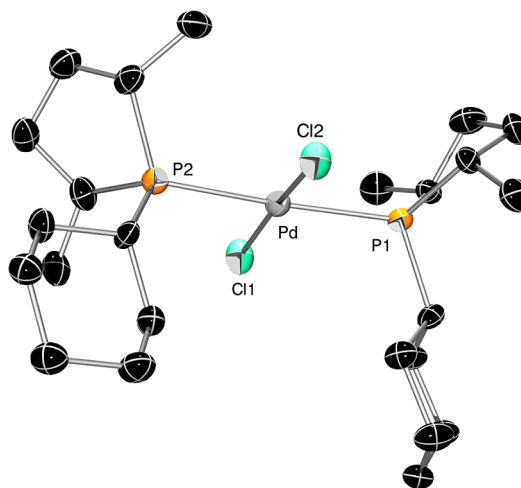


Figure 2. X-ray structure of complex **9c**. The thermal ellipsoids are displayed at 50% probability, and hydrogen atoms are omitted for clarity. Selected bond lengths (Å) and angles (deg): P1–Pd, 2.3428(14); P2–Pd, 2.3226(15); Cl1–Pd, 2.2899(15); Cl2–Pd, 2.3089(14); P1–Pd–P2, 176.69(5); Cl1–Pd–Cl2, 171.95(6); P1–Pd–Cl1, 92.04(6); P1–Pd–Cl2, 90.04(5); P2–Pd–Cl1, 90.90(6); P2–Pd–Cl2, 87.25(4).

The influence of the different phosphine substituents (*t*Bu, Cy, and *i*Pr) can be visualized from the X-ray structures. For instance, this group occupies the space below the complex plane. The larger this group becomes with respect to the C_2 -symmetric phospholane unit, the more a reaction at the metal center will be influenced by this chiral environment. Remarkably, these differences become most apparent with the smallest congener, methyl-substituted phospholane derivative **6a**, which yielded the palladium(II) complex **9a**, crystallizing as its cis isomer (Figure 4). However, in solution either the trans

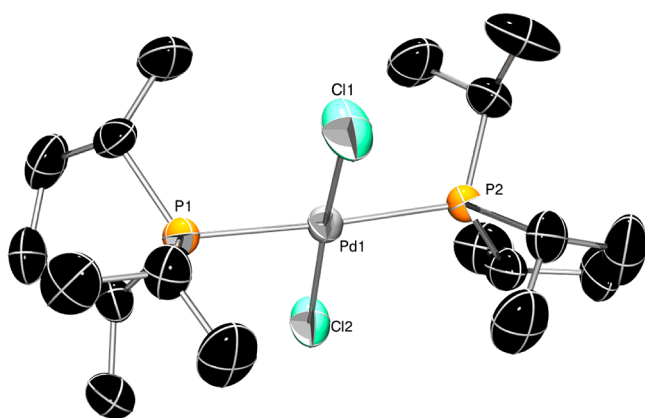


Figure 3. X-ray structure of complex **9b**. The thermal ellipsoids are displayed at 50% probability, and hydrogen atoms are omitted for clarity. Selected bond lengths (Å) and angles (deg): P1–Pd, 2.3296(8); P2–Pd, 2.3209(8); Cl1–Pd, 2.3058(10); Cl2–Pd, 2.2929(9); P1–Pd–P2, 176.54(3); Cl1–Pd–Cl2, 174.08(4); P1–Pd–Cl1, 88.83(4); P1–Pd–Cl2, 91.80(3); P2–Pd–Cl1, 88.27(3); P2–Pd–Cl2, 91.28(3).

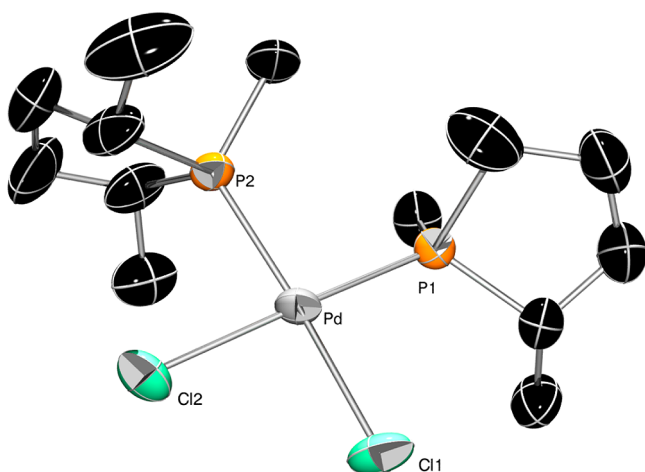


Figure 4. X-ray structure of complex **9a**. The thermal ellipsoids are displayed at 50% probability, and hydrogen atoms are omitted for clarity. Selected bond lengths (Å) and angles (deg): P1–Pd, 2.2611(15); P2–Pd, 2.2710(15); Cl1–Pd, 2.3624(15); Cl2–Pd, 2.3589(16); P1–Pd–P2, 93.98(5); Cl1–Pd–Cl2, 89.68(6); P1–Pd–Cl1, 90.96(5); P1–Pd–Cl2, 173.56(6); P2–Pd–Cl1, 174.16(6); P2–Pd–Cl2, 85.75(6).

isomer (CDCl_3) is more stable or a mixture between *cis* and *trans* isomers (CD_3CN) can be observed. In contrast, the corresponding nickel(II) complex **10**, ligated as well with **6a**, restores the expected *trans* geometry (Figure 5).

Steric and Electronic Properties of the Ligands. From the X-ray crystallographic data of the complexes, the buried volumes ($\%V_{\text{bur}}$) for the synthesized phosphines were calculated using SambVca¹⁷ to assess the steric bulk of the ligands **6**.¹⁸ The smallest derivative, **6a**, has a buried volume between 25.5 and 26% (Table 1, entry 4). The larger *iPr* and *Cy* derivatives are expectably relatively similar and have $\%V_{\text{bur}}$ values of between 29.3 and 29.8 for **6c** and between 29.1 and 29.2 for **6d**. The value for the *tert*-butyl derivative **6e** was determined to be between 29.8 and 30.9 (entry 8). We next aimed to compare the steric and electronic properties of the free phosphines derived from **6a–e** with those of some of their underlying achiral versions. For this purpose, the carbonyl

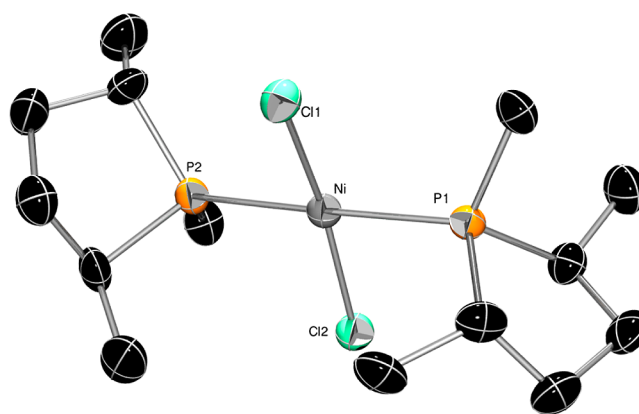


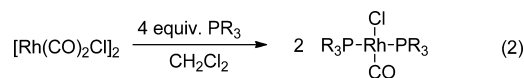
Figure 5. X-ray structure of nickel(II) complex **10**. The thermal ellipsoids are displayed at 50% probability, and hydrogen atoms are omitted for clarity. Selected bond lengths (Å) and angles (deg): Ni–P1, 2.230(2); Ni–P2, 2.244(2); Ni–Cl1, 2.178(2); Ni–Cl2, 2.177(2); P1–Ni–P2, 176.50(8); Cl1–Ni–Cl2, 168.83(9); P1–Ni–Cl1, 89.28(9); P1–Ni–Cl2, 89.95(9); P2–Ni–Cl1, 92.05(9); P2–Ni–Cl2, 89.28(9).

Table 1. Buried Volume (Pd Complexes) and CO Stretching Frequencies (Rh Complexes) of the Ligands

| entry | ligand L | $\%V_{\text{bur}}^a$ | $\nu(\text{CO}_{\text{Rh}})$ (cm^{-1}) ^b |
|-------|-------------------|----------------------|--|
| 1 | PCy ₃ | 31.8 ^c | 1940 (1943) ^d |
| 2 | PtBu ₃ | 36.7 ^c | |
| 3 | PBu ₃ | 25.9 ^c | 1955 ^d |
| 4 | 6a | 25.5; 26.0 | 1946 |
| 5 | 6b | | 1951 |
| 6 | 6c | 29.3; 29.8 | 1939 (1947) ^e |
| 7 | 6d | 29.1; 29.2 | 1944 |
| 8 | 6e | 29.8; 30.9 | 1941 |
| 9 | 8 | | 1942 |

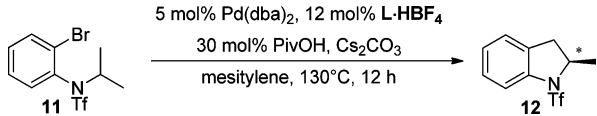
^aCalculated for both crystallographically independent ligands according to ref 17. ^bCO stretching frequencies for the *trans*-[RhCl(CO)-(PR₃)₂] complexes; ATR measurements on a Bruker ALPHA FT-IR spectrometer. ^cData from ref 18, calculated from the free phosphine. ^dData from ref 19. ^eData from ref 11a.²⁰

stretching frequencies of the corresponding rhodium complexes [(PR₃)₂Rh(CO)Cl], which are readily prepared from [Rh(CO)₂Cl]₂, were used (eq 2).



The carbonyl stretching frequencies of these complexes are a commonly used indicator of the donor abilities of the respective phosphine.¹⁹ The measured values match very well with tricyclohexylphosphine as prototype for an electron-rich trialkylphosphine (Table 1). Only the benzyl derivative **6b** (entry 5) is slightly less electron rich, placing it in the range of tributylphosphine.

Catalytic C(sp³)-H Functionalization. For a brief initial assessment of this class of ligands for potential application in asymmetric transition-metal catalysis, we evaluated them in the challenging C(sp³)-H functionalization of aniline derivative **11** to provide indoline **12** (Table 2). This transformation has recently been studied by several groups,²¹ including ours.⁸ We reported that **L4** works excellently with aryl triflates, whereas the corresponding aryl bromides were less reactive. In contrast,

Table 2. Evaluation of the Phosphines **6a–e** and **8** in C(sp³)–H Bond Functionalizations of **11**^a


| entry | L-HBF ₄ | yield (%) ^b | er ^c |
|-------|-----------------------------|------------------------|-----------------|
| 1 | 6a -HBF ₄ | 68 ^d | 55.5:44.5 |
| 2 | 6b -HBF ₄ | traces ^d | |
| 3 | 6c -HBF ₄ | 97 | 61:39 |
| 4 | 6d -HBF ₄ | 91 | 55.5:44.5 |
| 5 | 6e -HBF ₄ | 96 | 85.5:14.5 |
| 6 | 8 -HBF ₄ | 89 | 43:57 |

^aReaction conditions: 0.06 mmol of **11**, 7.20 μmol of L-HBF₄, 3.00 μmol of Pd(dba)₂, 18 μmol of PivOH, 1.5 equiv of Cs₂CO₃, 0.3 M in mesitylene at 130 °C for 12 h. ^bYield of isolated product **12**. ^cDetermined by HPLC using a chiral stationary phase. ^dThe reaction did not reach full conversion.

the developed electron-rich phospholanes **6a–e** and **8** successfully promoted this test transformation, displaying a reverse preference. The benzyl derivative **6b** did not catalyze the reaction (entry 2), presumably undergoing a cyclometalation of the ligand leading to an incompetent species. Increasing the bulk of the alkyl substituent led to more active catalysts as well as higher enantioselectivities (entry 1 vs entries 3–5). In this respect, ligand **6e**, bearing a bulky *tert*-butyl group proved to be the best, affording **12** in 96% yield and 85.5:14.5 enantiomeric ratio (entry 5). In contrast with our previous report,⁸ the isopropyl substituent on the phospholane module was not beneficial for the selectivity (entry 6).

CONCLUSIONS

In summary, we have reported a class of electron-rich trialkylphosphine ligands which incorporate the chiral phospholane moiety. These ligands have a low molecular weight, and even the bulkiest congener comes more closely to the steric and electronic properties of tricyclohexylphosphine and to those of tri-*tert*-butylphosphine. We demonstrated that they are able to induce selectivity in C(sp³)–H bond functionalization at high reaction temperatures.

EXPERIMENTAL SECTION

Chemicals and Reagents. All manipulations were carried out under an inert N₂(g) atmosphere using standard Schlenk or glovebox techniques. Solvents were purified using a two-column solid-state purification system (Innovative Technology, Amesbury, MA) and degassed prior to use with three pump–freeze–thaw cycles. Unless otherwise noted, all other reagents and starting materials were purchased from commercial sources and used without further purification. (*S,S*)-1-Chloro-2,5-dimethylphospholane (**5**)¹² was prepared as previously reported.

Physical Methods. The ¹H, ¹³C{¹H}, and ³¹P{¹H} NMR spectra were recorded at 293 K on a Bruker Avance 400 spectrometer. HPLC analyses were conducted on an Agilent 1260 Analytical HPLC system equipped with a Daicel Chiralcel (Chiralpak) OZH column. Elemental analyses were performed on a Carlo Erba EA 1110 CHN instrument at EPFL. X-ray diffraction studies were carried out at the EPFL Crystallography Facility. The data collections for the crystal structures were performed at low temperature using Mo K α radiation on a Bruker APEX II CCD diffractometer equipped with a κ geometry goniometer. The data were reduced by EvalCCD²² and then corrected for absorption.²³ The solution and refinement was performed by SHELX.²⁴ The structure was refined using full-matrix least squares

based on F² with all non-hydrogen atoms anisotropically defined. Hydrogen atoms were placed in calculated positions by means of the “riding” model.

General Procedure for the Synthesis of the Alkylphospholane-HBF₄ Compounds. To a mixture of **5** (301 mg, 2 mmol), CuBr-SMe₂ (20 mg, 0.1 mmol), and LiBr (17 mg, 0.2 mmol) in *n*-hexane (4 mL) was added dropwise a solution of the alkyl Grignard reagent (2.4 mmol) at 0 °C. The reaction mixture was stirred at 23 °C overnight, cooled to 0 °C, and quenched with degassed aqueous 3 M HBF₄ (6.6 mL, 20 mmol). The biphasic mixture was stirred for 15 min at 23 °C. The aqueous layer was separated, washed with *n*-hexane (2 × 5 mL), and extracted with DCM (3 × 20 mL). Combined DCM extracts were dried (MgSO₄) and concentrated in vacuo, yielding crude phosphine salts which subsequently were purified as stated below.

(2*S*,5*S*)-1,2,5-Trimethylphospholan-1-ium Tetrafluoroborate (6a**-HBF₄).** Prepared from 3.2 M (2-MeTHF) MeMgBr (0.75 mL). Recrystallized from a minimum amount of boiling MeOH (ca. 0.5 mL), after cooling to 0 °C. Yield: 166 mg (38%), white solid. ¹H NMR (400 MHz, CDCl₃, δ): 6.27 (dm, *J*_{PH} = 501.8 Hz, 1H), 3.06–3.21 (m, 1H), 2.51–2.65 (m, 1H), 2.25–2.50 (m, 2H), 1.96 (dd, *J*₁ = 15.4 Hz, *J*₂ = 5.7 Hz, 3H), 1.58–1.77 (m, 2H), 1.52 (dd, *J*₁ = 19.8 Hz, *J*₂ = 7.1 Hz, 3H), 1.39 (dd, *J*₁ = 18.6 Hz, *J*₂ = 7.3 Hz, 3H). ¹³C{¹H} NMR (100 MHz, CDCl₃, δ): 34.14 (d, *J* = 7.1 Hz), 33.55 (d, *J* = 7.9 Hz), 31.48 (d, *J* = 49.8 Hz), 27.56 (d, *J* = 49.1 Hz), 15.03 (d, *J* = 1.7 Hz), 13.16 (d, *J* = 2.5 Hz), –0.22 (d, *J* = 45.6 Hz). ³¹P{¹H} NMR (162 MHz, CDCl₃, δ): 33.2. IR (ATR, cm⁻¹): 3011, 2934, 2888, 1462, 1418, 1390, 1311, 1286, 1048, 1038, 950, 916, 840, 811, 792, 763. HRMS (ESI): calcd for [M – BF₄]⁺ 131.0984, found 131.0985. [α]_D²⁰ = –17.3° (*c* = 0.5, MeCN). Mp: 225–227 °C.

(2*S*,5*S*)-1-Benzyl-2,5-dimethylphospholan-1-ium Tetrafluoroborate (6b**-HBF₄).** Prepared from 1.5 M (THF) BnMgCl (1.6 mL). Recrystallized from a minimum amount of boiling EtOH (ca. 7 mL), after cooling to 0 °C. Yield: 267 mg (45%), yellowish solid. ¹H NMR (400 MHz, CD₃CN, δ): 7.38–7.49 (m, 5H), 5.97 (dm, *J*_{PH} = 488.4 Hz, 1H), 3.83 (t, *J* = 15.6 Hz, 1H), 3.58 (td, *J*₁ = 14.9 Hz, *J*₂ = 10.9 Hz, 1H), 2.93–3.07 (m, 1H), 2.57–2.72 (m, 1H), 2.20–2.46 (m, 2H), 1.60–1.73 (m, 1H), 1.47–1.59 (m, 1H), 1.39 (dd, *J*₁ = 18.1 Hz, *J*₂ = 7.3 Hz, 3H), 0.88 (dd, *J*₁ = 18.8 Hz, *J*₂ = 7.1 Hz, 3H). ¹³C{¹H} NMR (100 MHz, CD₃CN, δ): 130.72 (d, *J* = 3.0 Hz), 130.53 (d, *J* = 5.8 Hz), 129.63 (d, *J* = 3.6 Hz), 129.47 (d, *J* = 9.5 Hz), 34.87 (d, *J* = 6.7 Hz), 34.24 (d, *J* = 7.6 Hz), 31.11 (d, *J* = 48.5 Hz), 30.04 (d, *J* = 43.5 Hz), 22.79 (d, *J* = 38.7 Hz), 15.45 (d, *J* = 3.1 Hz), 13.39 (d, *J* = 2.5 Hz). ³¹P{¹H} NMR (162 MHz, CD₃CN, δ): 39.7. IR (ATR, cm⁻¹): 3639, 2972, 2940, 2880, 2112, 1602, 1497, 1456, 1408, 1388, 1284, 1237, 1052, 931, 862, 791, 766, 739, 702.81. HRMS (ESI): calcd for [M – BF₄]⁺ 207.1297, found 207.1291. [α]_D²⁰ = –72.7° (*c* = 0.5, MeCN). Mp: 169–170 °C.

(2*S*,5*S*)-1-Isopropyl-2,5-dimethylphospholan-1-ium Tetrafluoroborate (6c**-HBF₄).** Prepared from 1.3 M (THF) *i*PrMgCl (1.85 mL). Recrystallized from EtOH (ca. 0.5 mL), after cooling to –30 °C. Yield: 361 mg (73%), white solid. ¹H NMR (400 MHz, CD₃CN, δ): 5.72 (dq, *J*_{1(PH)}} = 474.1 Hz, *J*₂ = 6.4 Hz, 1H), 2.92–3.07 (m, 1H), 2.67–2.83 (m, 2H), 2.24–2.42 (m, 2H), 1.52–1.68 (m, 2H), 1.33–1.46 (m, 12H). ¹³C{¹H} NMR (100 MHz, CD₃CN, δ): 35.47 (d, *J* = 6.4 Hz), 34.14 (d, *J* = 6.1 Hz), 30.16 (d, *J* = 44.1 Hz), 28.86 (d, *J* = 45.8 Hz), 19.53 (d, *J* = 38.6 Hz), 18.28 (d, *J* = 3.0 Hz), 16.94 (d, *J* = 3.1 Hz), 16.46 (d, *J* = 2.5 Hz), 13.07 (d, *J* = 2.5 Hz). ³¹P{¹H} NMR (162 MHz, CD₃CN, δ): 46.62. IR (ATR, cm⁻¹): 2973, 2940, 2881, 1462, 1391, 1284, 1047, 932, 892, 856, 804, 709.92. HRMS (ESI): calcd for [M – BF₄]⁺ 159.1297, found 159.1299. [α]_D²⁰ = –11.3° (*c* = 0.5, MeCN). Mp: 182–183 °C.

(2*S*,5*S*)-1-Cyclohexyl-2,5-dimethylphospholan-1-ium Tetrafluoroborate (6d**-HBF₄).** Prepared from 1 M (THF) CyMgBr (2.4 mL). Dissolved in a minimum amount of DCM (ca. 0.3 mL) and layered with *n*-pentane (5 mL). Yield: 203 mg (51%), white solid. ¹H NMR (400 MHz, CD₃CN, δ): 5.83 (dq, *J*_{1(PH)}} = 476.1 Hz, *J*₂ = 6.5 Hz, 1H), 3.09–3.24 (m, 1H), 2.59–2.87 (m, 2H), 2.28–2.45 (m, 2H), 2.06–2.17 (m, 1H), 1.82–2.04 (m, 3H), 1.61–1.81 (m, 3H), 1.39–1.56 (m, 10H), 1.23–1.36 (m, 1H). ¹³C{¹H} NMR (100 MHz, CDCl₃, δ):

35.04 (d, $J = 6.4$ Hz), 33.62 (d, $J = 6.1$ Hz), 29.36 (d, $J = 43.6$ Hz), 28.40 (d, $J = 3.6$ Hz), 28.04 (d, $J = 45.8$ Hz), 27.57 (d, $J = 37.3$ Hz), 27.03 (d, $J = 3.8$ Hz), 25.87 (d, $J = 13.4$ Hz), 25.72 (d, $J = 13.4$ Hz), 25.15 (d, $J = 1.4$ Hz), 16.48 (d, $J = 2.0$ Hz), 13.09 (d, $J = 1.9$ Hz). $^{31}\text{P}\{^1\text{H}\}$ NMR (162 MHz, CDCl_3 , δ): 42.50. IR (ATR, cm^{-1}): 3627, 3558, 2936, 2860, 1633, 1451, 1389, 1283, 1053, 908. HRMS (ESI): calcd for $[\text{M} - \text{BF}_4]^+$ 199.1610, found 199.1609. $[\alpha]_{\text{D}}^{20} = -9.3^\circ$ ($c = 0.5$, MeCN). Mp: 65–66 °C.

(2*S*,5*S*)-1-(*tert*-Butyl)-2,5-dimethylphospholan-1-ium Tetrafluoroborate (6e-HBF₄). Prepared from 2 M (Et_2O) *t*BuMgCl (1.2 mL). Recrystallized from a minimum amount of boiling EtOH (ca. 1 mL), after cooling to 0 °C. Yield: 282 mg (54%), white solid. ^1H NMR (400 MHz, CD_3CN , δ): 5.68 (dm, $J_{\text{PH}} = 468.7$ Hz, 1H), 2.95–3.10 (m, 1H), 2.75–2.90 (m, 1H), 2.24–2.42 (m, 2H), 1.54–1.73 (m, 2H), 1.49 (dd, $J_1 = 13.5$ Hz, $J_2 = 7.2$ Hz, 3H), 1.45 (dd, $J_1 = 15.2$ Hz, $J_2 = 7.2$ Hz, 3H), 1.43 (d, $J = 17.1$ Hz, 9H). $^{13}\text{C}\{^1\text{H}\}$ NMR (100 MHz, CD_3CN , δ): 36.06 (d, $J = 6.8$ Hz), 33.90 (d, $J = 4.8$ Hz), 32.51 (d, $J = 40.0$ Hz), 31.23 (d, $J = 36.1$ Hz), 29.04 (d, $J = 44.6$ Hz), 26.12, 17.22 (d, $J = 2.9$ Hz), 13.48 (d, $J = 2.6$ Hz). $^{31}\text{P}\{^1\text{H}\}$ NMR (162 MHz, CD_3CN , δ): 49.7. IR (ATR, cm^{-1}): 3631, 2972, 1626, 1465, 1408, 1377, 1283, 1203, 1051, 932, 895, 813, 763, 678, 665. HRMS (ESI): calcd for $[\text{M} - \text{BF}_4]^+$ 173.1454, found 173.1454. $[\alpha]_{\text{D}}^{20} = -5.3^\circ$ ($c = 0.3$, MeCN). Mp: 199–204 °C.

(2*R*,5*R*)-1-Cyclohexyl-2,5-diisopropylphospholan-1-ium Tetrafluoroborate (8-HBF₄). Cyclohexylphosphine (28.4 mg, 0.25 mmol) was weighed into a glovebox into a flame-dried reaction tube, dissolved in THF (1 mL), and cooled to –78 °C. A 1.6 M solution (hexane) of BuLi (0.23 mL, 0.37 mmol) was added dropwise, and the solution was warmed to 23 °C and stirred for 1 h. The reaction mixture was cooled to –78 °C, and a solution of (4*S*,7*S*)-4,7-diisopropyl-1,3,2-dioxathiepane 2,2-dioxide (59.1 mg, 0.25 mmol) in THF (0.5 mL) was added dropwise. The reaction mixture was warmed to 23 °C, stirred for 4 h, and cooled to –78 °C. A 1.6 M solution (hexane) of BuLi (0.23 mL, 0.37 mmol) was added dropwise, and then the reaction mixture was slowly warmed to 23 °C and stirred overnight. A 1 M (THF) $\text{BH}_3 \cdot \text{THF}$ (0.750 mL, 0.750 mmol) was added at 0 °C, and the reaction mixture was stirred for 1 h at room temperature. Then 1 M HCl was added at 0 °C. The reaction mixture was diluted with pentane. The layers were separated, and the organic layer was further washed with water (x2) and dried over MgSO_4 . The crude mixture was purified by chromatography on silica gel column using hexane/ Et_2O 30/1 as eluent to afford BH_3 -protected (2*R*,5*R*)-1-cyclohexyl-2,5-diisopropylphospholane (40.2 mg, 0.15 mmol, 61% yield) as a colorless oil. This oil was dissolved under nitrogen in 4.0 mL of dry and degassed DCM and cooled to 0 °C, and diethyloxonium tetrafluoroborate (0.31 mL, 2.24 mmol) was added dropwise. The reaction mixture was stirred at 0 °C for 30 min and then 30 min at 23 °C. Degassed 8.0 M hydrogen tetrafluoroborate (1.90 mL, 14.9 mmol) was added at 23 °C, and the reaction mixture was vigorously stirred for 30 min. The aqueous phase was washed with DCM (3 × 10 mL). The combined organic layers were dried over MgSO_4 , and DCM was removed in vacuo to afford 8-HBF₄ as a white solid (50.1 mg, 0.15 mmol, 98% yield). ^1H NMR (400 MHz, CDCl_3 , δ): 6.51 (d, $J_{\text{PH}} = 486.7$ Hz, 1H), 2.86–2.69 (m, 1H), 2.59–2.32 (m, 4H), 2.28–2.08 (m, 2H), 2.06–1.68 (m, 6H), 1.62–1.38 (m, 5H), 1.35–1.27 (m, 1H), 1.26 (d, $J = 6.6$ Hz, 3H), 1.14 (d, $J = 6.8$ Hz, 3H), 1.12 (d, $J = 6.8$ Hz, 3H), 1.09 (d, $J = 6.6$ Hz, 3H). $^{13}\text{C}\{^1\text{H}\}$ NMR (100 MHz, CDCl_3 , δ): 44.3 (d, $J = 41.5$ Hz), 40.2 (d, $J = 44.6$ Hz), 31.3 (d, $J = 7.8$ Hz), 30.2 (d, $J = 1.8$ Hz), 30.0 (d, $J = 5.1$ Hz), 28.5 (d, $J = 37.5$ Hz), 28.5 (d, $J = 3.6$ Hz), 28.0 (d, $J = 3.8$ Hz), 27.5 (d, $J = 1.7$ Hz), 26.3 (d, $J = 13.5$ Hz), 25.9 (d, $J = 12.9$ Hz), 25.0 (d, $J = 1.7$ Hz), 24.0 (d, $J = 2.7$ Hz), 23.6 (d, $J = 5.2$ Hz), 21.7 (d, $J = 12.1$ Hz), 20.9 (d, $J = 10.8$ Hz). $^{31}\text{P}\{^1\text{H}\}$ NMR (162 MHz, CDCl_3 , δ): 27.0. IR (ATR, cm^{-1}): 2965, 2938, 2860, 2435, 1449, 1051, 518. HRMS (ESI): calcd for $[\text{M} - \text{BF}_4]^+$ 255.2236, found 255.2237. $[\alpha]_{\text{D}}^{20} = -71.0^\circ$ ($c = 0.35$, CHCl_3). Mp: 202–203 °C.

General Procedure for the Synthesis of the Palladium Complexes.²⁵ Phosphine salt 6-HBF₄ (0.5 mmol) and powdered Na_2CO_3 (106 mg, 1 mmol) were suspended in MeOH (1.5 mL). The mixture was sonicated at 23 °C for 30 min and filtered in the glovebox.

The filtrate was added dropwise to a vigorously stirred solution of K_2PdCl_4 (65 mg, 0.2 mmol) in degassed H_2O (1.5 mL) at 23 °C. After the mixture was stirred for 30 min, the brown-yellow precipitate was collected on a filter, washed successively with H_2O (2 × 0.5 mL) and MeOH (2 × 0.2 mL), and dried in vacuo. In order to remove any Pd metal, the obtained powder was dissolved in DCM (1 mL) and filtered through Celite. The filtrate was evaporated with EtOH in vacuo, yielding pure Pd complex.

Complex 9a. Prepared from 6a-HBF₄ (109 mg). Yield: 48 mg (55%), light yellow needles. ^1H NMR (400 MHz, CDCl_3 ; predominantly the trans isomer, δ): 3.20–3.33 (m, 2H), 2.26–2.37 (m, 2H), 2.07–2.23 (m, 4H), 1.61–1.76 (m, 3H), 1.46–1.57 (m, 13H), 1.25 (dd, $J_1 = 15.6$ Hz, $J_2 = 7.1$ Hz, 6H). $^{31}\text{P}\{^1\text{H}\}$ NMR (162 MHz, CDCl_3 , δ): 45.8 (trans), 28.8 (cis). IR (ATR, cm^{-1}): 2953, 2929, 2862, 1452, 1408, 1377, 1286, 1162, 1076, 1059, 1014, 886, 739.32. Anal. Found (calcd) for $\text{C}_{14}\text{H}_{30}\text{Cl}_2\text{P}_2\text{Pd}$: C, 38.46 (38.42); H, 6.97 (6.91). $[\alpha]_{\text{D}}^{20} = +134.6^\circ$ ($c = 0.5$, CHCl_3). Mp: 164–166 °C. Assignment of the trans/cis isomers of the complex 9a by ^{31}P spectra in different solvents: $^{31}\text{P}\{^1\text{H}\}$ NMR (162 MHz, C_6D_6 , δ) 28.6 (cis isomer, one peak only, sample is sparingly soluble); $^{31}\text{P}\{^1\text{H}\}$ NMR (162 MHz, CDCl_3 , δ) 45.8 and 28.8 (trans:cis ratio 92:8); $^{31}\text{P}\{^1\text{H}\}$ (162 MHz, CD_3CN , δ) 47.1 and 29.2 (trans:cis ratio: 83:17).

Complex 9b. Prepared from 6c-HBF₄ (123 mg). Yield: 67 mg (68%), bright yellow solid. ^1H NMR (400 MHz, CDCl_3 , δ): 2.98–3.13 (m, 2H), 2.36–2.53 (m, 4H), 1.98–2.15 (m, 4H), 1.28–1.62 (m, 28H). $^{31}\text{P}\{^1\text{H}\}$ NMR (162 MHz, CDCl_3 , δ): 44.7. IR (ATR, cm^{-1}): 2954, 2939, 2922, 2865, 1454, 1387, 1368, 1246, 1158, 1086, 1059, 1039, 883. Anal. Found (calcd) for $\text{C}_{18}\text{H}_{38}\text{Cl}_2\text{P}_2\text{Pd}$: C, 43.54 (43.78); H, 7.67 (7.76). $[\alpha]_{\text{D}}^{20} = +174.6^\circ$ ($c = 0.5$, CHCl_3). Mp: 152–153 °C.

Complex 9c. Prepared from 6d-HBF₄ (143 mg). Yield: 86 mg (82%), bright yellow solid. ^1H NMR (400 MHz, CDCl_3 , δ): 2.94–3.07 (m, 2H), 2.44–2.56 (m, 2H), 1.95–2.23 (m, 10H), 1.64–1.91 (m, 10H), 1.18–1.61 (m, 22H). $^{31}\text{P}\{^1\text{H}\}$ NMR (162 MHz, CDCl_3 , δ): 41.1. IR (ATR, cm^{-1}): 2926, 2852, 1447, 1374, 1174, 1159, 1076, 1003, 849, 733. Anal. Found (calcd) for $\text{C}_{24}\text{H}_{46}\text{Cl}_2\text{P}_2\text{Pd}$: C, 50.22 (50.23); H, 8.06 (8.08). $[\alpha]_{\text{D}}^{20} = +106.5^\circ$ ($c = 0.5$, CHCl_3). Mp: 123–124 °C.

Complex 9d. Prepared from 6e-HBF₄ (130 mg). Yield: 85 mg (74%), deep yellow solid. ^1H NMR (400 MHz, CDCl_3 , δ): 3.06–3.18 (m, 2H), 2.42–2.53 (m, 2H), 1.98–2.15 (m, 4H), 1.51–1.65 (m, 17H), 1.42–1.48 (m, 17H). $^{31}\text{P}\{^1\text{H}\}$ NMR (162 MHz, CDCl_3 , δ): 48.4; IR (ATR, cm^{-1}): 2991, 2948, 2928, 2894, 2865, 1461, 1451, 1365, 1182, 1157, 1072, 1016, 813.41. Anal. Found (calcd) for $\text{C}_{20}\text{H}_{42}\text{Cl}_2\text{P}_2\text{Pd}$: C, 45.95 (46.03); H, 8.21 (8.11). $[\alpha]_{\text{D}}^{20} = +116.0^\circ$ ($c = 0.5$, CHCl_3). Mp: 241–243 °C.

Synthesis of the Nickel Complexes 10. 6a-HBF₄ (218 mg, 1 mmol) and powdered Na_2CO_3 (212 mg, 2 mmol) were suspended in EtOH (1 mL). The mixture was sonicated at 23 °C for 30 min and filtered in the glovebox. $\text{NiCl}_2 \cdot \text{DME}$ (88 mg, 0.4 mmol) was dissolved with heating in EtOH (1 mL). The slightly turbid solution was filtered through Celite and added dropwise to the vigorously stirred solution of the phosphine. The resulting deep purple solution was refluxed for 15 min, cooled to 23 °C, and concentrated to a volume of ca. 0.5 mL. After standing at 23 °C overnight the mother liquor was removed and the residual deep purple crystalline solid was washed successively with cold MeOH (2 × 0.3 mL) and Et_2O (2 × 0.3 mL) and dried in vacuo. Yield: 86 mg (55%). ^1H NMR (400 MHz, C_6D_6 , δ): 2.8–2.94 (m, 2H), 2.04 (d, $J = 6.7$ Hz, 6H), 1.49–1.71 (m, 6H), 1.14–1.29 (m, 2H), 0.77–1.01 (m, 14H). $^{31}\text{P}\{^1\text{H}\}$ NMR (162 MHz, CDCl_3 , δ): 66.9. IR (ATR, cm^{-1}): 3369, 2964, 2930, 2862, 1452, 1411, 1376, 1288, 1162, 1075, 1059, 1015, 925, 888, 737. Anal. Found (calcd) for $\text{C}_{14}\text{H}_{30}\text{Cl}_2\text{P}_2\text{Ni}$: C, 43.41 (43.12); H, 8.12 (7.75). $[\alpha]_{\text{D}}^{20} = +60^\circ$ ($c = 0.5$, toluene). Mp: 101–102 °C.

Procedure for the Catalytic Reaction with Aryl Bromide 11. $\text{Pd}(\text{dba})_2$ (1.72 mg, 3.00 μmol), 6e-HBF₄ (1.87 mg, 12.0 μmol), 11 (20.8 mg, 0.06 mmol), PivOH (1.84 mg, 18.0 μmol), and Cs_2CO_3 (29.3 mg, 0.09 mmol) were weighed into a vial equipped with a magnetic stirrer bar and sealed with a rubber septum. The vial was put under vacuum and then backfilled with nitrogen (×3). Mesitylene (200 μL , 0.3 M) was added, and the mixture was degassed by three

freeze–pump–thaw cycles. The mixture was stirred at 23 °C for 1 h and then heated to 135 °C for 12 h, cooled to room temperature, and then directly purified on silica gel, yielding **12** as a colorless oil. The absolute configuration was assigned by comparison with the literature data.⁸ ¹H NMR (400 MHz, CDCl₃, δ): 7.48 (d, *J* = 7.7 Hz, 1H), 7.28–7.23 (m, 2H), 7.20–7.11 (m, 1H), 4.84–4.65 (m, 1H), 3.54 (dd, *J* = 15.9, 9.2 Hz, 1H), 2.74 (dd, *J* = 15.9, 1.7 Hz, 1H), 1.46 (d, *J* = 6.5 Hz, 3H) ppm. ¹³C{¹H} NMR (100 MHz, CDCl₃, δ): 138.4, 130.6, 128.1, 125.8, 125.5, 120.2 (q, *J*_{C–F} = 325.3 Hz), 115.7, 60.9, 36.3, 22.8 ppm. IR (ATR, cm^{−1}): 2986, 2930, 1597, 1480, 1462, 1395, 1327, 1254, 1224, 1188, 1144, 1102, 1027, 939, 752, 709, 649, 608, 575, 528 cm^{−1}. HRMS (EI): calcd. for [C₁₀H₁₀F₂NO₂S]⁺ 265.0379, found 265.0379. [α]_D²⁰ = 25.3 (*c* = 1.0, CHCl₃). *R*_f = 0.64 (pentane/EtOAc, 15/1). HPLC separation (Chiralpak OZH, 4.6 × 250 mm; 0.5% *i*-PrOH/hexane, 1.0 mL/min, 254 nm; *t*_r(minor) = 8.8 min, *t*_r(major) = 6.7 min): 85.5:14.5 er.

Crystallographic Details for 9a. A total of 7427 reflections ($-9 < h < 10$, $-14 < k < 12$, $-28 < l < 24$) were collected at *T* = 293(2) K in the range 3.13–29.28°, 4319 of which were unique (*R*_{int} = 0.0379), with Mo *K*α radiation (λ = 0.710 73 Å). The structure was solved by direct methods. All non-hydrogen atoms were refined anisotropically, and hydrogen atoms were placed in calculated idealized positions. The residual peak and hole electron densities were 0.611 and −0.741 e Å^{−3}, respectively. The absorption coefficient was 1.430 mm^{−1}. The least-squares refinement converged normally with residuals of *R*(*F*) = 0.0457 and *R*_w(*F*²) = 0.0732 and GOF = 1.049 (*I* > 2σ(*I*)). Crystal data for C₁₄H₃₀Cl₂P₂Pd: *M*_w = 437.62, space group *P*2₁2₁, orthorhombic, *a* = 8.0418(3) Å, *b* = 10.5872(4) Å, *c* = 22.0696(9) Å, α = 90°, β = 90°, γ = 90°, *V* = 1879.02(14) Å³, *Z* = 4, ρ_{calcd} = 1.547 Mg/m³.

Crystallographic Details for 9b. A total of 10 844 reflections ($-10 < h < 11$, $-11 < k < 16$, $-28 < l < 29$) were collected at *T* = 293(2) K in the range 2.92–29.29°, 5129 of which were unique (*R*_{int} = 0.0234), with Mo *K*α radiation (λ = 0.710 73 Å). The structure was solved by direct methods. All non-hydrogen atoms were refined anisotropically, and hydrogen atoms were placed in calculated idealized positions. The residual peak and hole electron densities were 0.555 and −0.481 e Å^{−3}, respectively. The absorption coefficient was 1.169 mm^{−1}. The least-squares refinement converged normally with residuals of *R*(*F*) = 0.0307 and *R*_w(*F*²) = 0.0541 and GOF = 1.049 (*I* > 2σ(*I*)). Crystal data for C₁₈H₃₈Cl₂P₂Pd: *M*_w = 493.72, space group *P*2₁2₁, orthorhombic, *a* = 8.5322(2) Å, *b* = 12.0949(3) Å, *c* = 22.4379(5) Å, α = 90°, β = 90°, γ = 90°, *V* = 2315.50(9) Å³, *Z* = 4, ρ_{calcd} = 1.416 Mg/m³.

Crystallographic Details for 9c. A total of 6684 reflections ($-11 < h < 11$, $-24 < k < 28$, $-11 < l < 11$) were collected at *T* = 140(2) K in the range 2.55–30.08°, 6684 of which were unique (*R*_{int} = 0.0000), with Mo *K*α radiation (λ = 0.710 73 Å). The structure was solved by direct methods. All non-hydrogen atoms were refined anisotropically, and hydrogen atoms were placed in calculated idealized positions. The residual peak and hole electron densities were 1.504 and −1.999 e Å^{−3}, respectively. The absorption coefficient was 1.014 mm^{−1}. The least-squares refinement converged normally with residuals of *R*(*F*) = 0.0658 and *R*_w(*F*²) = 0.1758 and GOF = 0.976 (*I* > 2σ(*I*)). Crystal data for C₂₄H₄₆Cl₂P₂Pd: *M*_w = 573.85, space group *P*2₁, monoclinic, *a* = 8.298(3) Å, *b* = 19.970(6) Å, *c* = 8.468(2) Å, α = 90°, β = 105.993(16)°, γ = 90°, *V* = 1348.9(7) Å³, *Z* = 2, ρ_{calcd} = 1.413 Mg/m³.

Crystallographic Details for 9d. A total of 33 297 reflections ($-10 < h < 11$, $-16 < k < 17$, $-28 < l < 29$) were collected at *T* = 293(2) K in the range 2.86–29.37°, 6272 of which were unique (*R*_{int} = 0.0345), with Mo *K*α radiation (λ = 0.710 73 Å). The structure was solved by direct methods. All non-hydrogen atoms were refined anisotropically, and hydrogen atoms were placed in calculated idealized positions. The residual peak and hole electron densities were 1.318 and −1.146 e Å^{−3}, respectively. The absorption coefficient was 1.082 mm^{−1}. The least-squares refinement converged normally with residuals of *R*(*F*) = 0.0533 and *R*_w(*F*²) = 0.1249 and GOF = 1.040 (*I* > 2σ(*I*)). Crystal data for C₂₀H₄₂Cl₂P₂Pd: *M*_w = 521.78, space group *P*2₁2₁, orthorhombic, *a* = 8.5030(3) Å, *b* = 13.0765(5) Å, *c* =

22.5786(8) Å, α = 90°, β = 90°, γ = 90°, *V* = 2510.49(16) Å³, *Z* = 4, ρ_{calcd} = 1.380 Mg/m³.

Crystallographic Details for 10. A total of 39 495 reflections ($-15 < h < 15$, $-16 < k < 16$, $-31 < l < 31$) were collected at *T* = 100(2) K in the range 3.29–27.50°, 8439 of which were unique (*R*_{int} = 0.1022), with Mo *K*α radiation (λ = 0.710 73 Å). The structure was solved by direct methods. All non-hydrogen atoms were refined anisotropically, and hydrogen atoms were placed in calculated idealized positions. The residual peak and hole electron densities were 1.433 and −1.346 e Å^{−3}, respectively. The absorption coefficient was 1.461 mm^{−1}. The least-squares refinement converged normally with residuals of *R*(*F*) = 0.0638 and *R*_w(*F*²) = 0.1619 and GOF = 1.065 (*I* > 2σ(*I*)). Crystal data for C₁₄H₃₀Cl₂NiP₂: *M*_w = 389.93, space group *P*2₁2₁, orthorhombic, *a* = 12.373(4) Å, *b* = 12.529(2) Å, *c* = 24.461(5) Å, α = 90°, β = 90°, γ = 90°, *V* = 3791.8(15) Å³, *Z* = 8, ρ_{calcd} = 1.366 Mg/m³.

■ ASSOCIATED CONTENT

📄 Supporting Information

Figures giving NMR spectra of all new compounds and HPLC traces for **12** and CIF files giving crystallographic data for **9a–d** and **10**. This material is available free of charge via the Internet at <http://pubs.acs.org>. CCDC 900820–900824 also contain the supplementary crystallographic data for **9a–d** and **10**. These data can be obtained free of charge from The Cambridge Crystallographic Data Centre via www.ccdc.cam.ac.uk/data_request/cif.

■ AUTHOR INFORMATION

Corresponding Author

*E-mail: nicolai.cramer@epfl.ch.

Notes

The authors declare no competing financial interest.

Biography



Nicolai Cramer was born in 1977 in Stuttgart, Germany. He studied chemistry at the University of Stuttgart (1998–2003) and obtained his Ph.D. from the same institution (2005; advisor Prof. Sabine Laschat). After a postdoctoral stint at Stanford (advisor Prof. Barry M. Trost), he started in 2007 his independent career as a habilitant at the chair of Prof. Erick M. Carreira at ETH Zurich, Switzerland. In 2010, he assumed his current position as assistant professor at the Ecole Polytechnique Fédérale de Lausanne (EPFL). His research interests encompass asymmetric catalysis, selective C–H and C–C bond functionalizations, and synthesis of bioactive natural products.

ACKNOWLEDGMENTS

This work was supported by the EPFL and by the European Research Council under the European Community's Seventh Framework Program (FP7 2007–2013)/ERC Grant agreement No. 257891. We thank Dr. R. Scopelliti for X-ray crystallographic analyses and Dr. R. Kadyrov (Evonik Industries AG) for generous donations of 2,5-dimethyl-1-TMS-phospholane.

REFERENCES

- (1) Knowles, W. S.; Sabacky, M. J.; Vineyard, B. D. *J. Chem. Soc., Chem. Commun.* **1972**, 10–11.
- (2) (a) Minnaard, A. J.; Feringa, B. L.; Lefort, L.; de Vries, J. G. *Acc. Chem. Res.* **2007**, *40*, 1267–1277. (b) Feringa, B. L. *Acc. Chem. Res.* **2000**, *33*, 346–353. (c) Reetz, M. T. *Angew. Chem., Int. Ed.* **2008**, *47*, 2556–2588.
- (3) Sometimes, they become bidentate ligands formed through in situ cyclometalation. For example, see: Hartwig, J. F.; Stanley, L. M. *Acc. Chem. Res.* **2010**, *43*, 1461–1475.
- (4) (a) Alexakis, A.; Vastra, J.; Burton, J.; Benhaim, C.; Mangeney, P. *Tetrahedron Lett.* **1998**, *39*, 7869–7872. (b) Keller, E.; Maurer, J.; Naasz, R.; Schader, T.; Meetsma, A.; Feringa, B. L. *Tetrahedron: Asymmetry* **1998**, *9*, 2409–2413.
- (5) (a) Hayashi, T. *Acc. Chem. Res.* **2000**, *33*, 354–362. (b) Yin, J.; Buchwald, S. L. *J. Am. Chem. Soc.* **2000**, *122*, 12051–12052. (c) Gladiali, S.; Dore, A.; Fabbri, D.; De Lucchi, O.; Manassero, M. *Tetrahedron: Asymmetry* **1994**, *5*, 511–514. (d) Chi, Y.; Zhang, X. *Tetrahedron Lett.* **2002**, *43*, 4849–4852. (e) Junge, K.; Oehme, G.; Monsees, A.; Riermeier, T.; Dingerdissen, U.; Beller, M. *Tetrahedron Lett.* **2002**, *43*, 4977–4980. (f) Enthaler, S.; Erre, G.; Junge, K.; Michalik, D.; Spannenberg, A.; Marras, F.; Gladiali, S.; Beller, M. *Tetrahedron: Asymmetry* **2007**, *18*, 1288–298. (g) Kollar, L.; Keglevich, G. *Chem. Rev.* **2010**, *110*, 4257–4302.
- (6) (a) Kündig, E. P.; Seidel, T. M.; Jia, Y.-X.; Bernardinelli, G. *Angew. Chem., Int. Ed.* **2007**, *46*, 8484–8487. (b) Würtz, S.; Lohre, C.; Fröhlich, R.; Bergander, K.; Glorius, F. *J. Am. Chem. Soc.* **2009**, *131*, 8344–8345. (c) Nakanishi, M.; Katayev, D.; Besnard, C.; Kündig, E. P. *Angew. Chem., Int. Ed.* **2011**, *50*, 7438–7441.
- (7) (a) Seiser, T.; Cramer, N. *Angew. Chem., Int. Ed.* **2008**, *47*, 9294–9297. (b) Seiser, T.; Roth, O. A.; Cramer, N. *Angew. Chem., Int. Ed.* **2009**, *48*, 6320–6323. (c) Albicker, M.; Cramer, N. *Angew. Chem., Int. Ed.* **2009**, *48*, 9139–9142. (d) Waibel, M.; Cramer, N. *Angew. Chem., Int. Ed.* **2010**, *49*, 4455–4458. (e) Seiser, T.; Cramer, N. *Chem. Eur. J.* **2010**, *16*, 3383–3391. (f) Seiser, T.; Cramer, N. *J. Am. Chem. Soc.* **2010**, *132*, 5340–5342. (g) Tran, D. N.; Cramer, N. *Angew. Chem., Int. Ed.* **2010**, *49*, 8181–8184. (h) Seiser, T.; Cramer, N. *Angew. Chem., Int. Ed.* **2010**, *49*, 10163–10167. (i) Waibel, M.; Cramer, N. *Chem. Commun.* **2011**, 345–348. (j) Tran, D. N.; Cramer, N. *Angew. Chem., Int. Ed.* **2011**, *50*, 11098–11102.
- (8) Saget, T.; Lémouzy, S.; Cramer, N. *Angew. Chem., Int. Ed.* **2012**, *51*, 2238–2242.
- (9) (a) Surry, D. S.; Buchwald, S. L. *Angew. Chem., Int. Ed.* **2008**, *47*, 6338–6361. (b) Martin, R.; Buchwald, S. L. *Acc. Chem. Res.* **2008**, *41*, 1461–1473. (c) Surry, D. S.; Buchwald, S. L. *Chem. Sci.* **2011**, *2*, 27–50.
- (10) (a) Burk, M. J. *Acc. Chem. Res.* **2000**, *33*, 363–372. (b) Lennon, I. C.; Pilkington, C. J. *Synthesis* **2003**, 1639–1642. (c) Guillen, F.; Fiaud, J.-C. *Tetrahedron Lett.* **1999**, *40*, 2939–2942. (d) Holz, J.; Monsees, A.; Jiao, H.; You, J.; Komarov, I. V.; Fischer, C.; Drauz, K.; Börner, A. *J. Org. Chem.* **2003**, *68*, 1701–1707. (e) Bonnaventure, I.; Charette, A. B. *J. Org. Chem.* **2008**, *73*, 6330–6340.
- (11) (a) Krüger, P.; Werner, H. *Eur. J. Inorg. Chem.* **2004**, 481–491. (b) Ohashi, A.; Matsukawa, S.; Imamoto, T. *Heterocycles* **2000**, *52*, 905–910.
- (12) Holz, J.; Monsees, A.; Kadyrov, R.; Börner, A. *Synlett* **2007**, 599–60201.
- (13) (a) Saget, T.; Cramer, N. *Synthesis* **2011**, 2369–2371. (b) Netherton, M. R.; Fu, G. C. *Org. Lett.* **2001**, *3*, 4295–4298.
- (14) Burk, M. J.; Feaster, J. E.; Nugent, W. A.; Harlow, R. L. *J. Am. Chem. Soc.* **1993**, *115*, 10125–10138.
- (15) Denmark, S. E.; Werner, N. S. *Org. Lett.* **2011**, *13*, 4596–4599.
- (16) Complexation experiments with **6b** with palladium(II) salts were not attempted due to the cyclometalation propensity of the benzyl substituent.
- (17) Poater, A.; Cosenza, B.; Correa, A.; Giudice, S.; Ragone, F.; Scarano, V.; Cavallo, L. *Eur. J. Inorg. Chem.* **2009**, 1759–1766. Parameters used for SambVca calculations: (i) for %Vbur calculations, 3.50 Å was selected as the value for the sphere radius; (ii) 2.28 Å was considered as the distance for the metal–ligand bond; (iii) hydrogen atoms were omitted; (iv) scaled Bondi radii were used.
- (18) Clavier, H.; Nolan, S. P. *Chem. Commun.* **2010**, 46, 841–861.
- (19) Roodt, A.; Otto, S.; Steyl, G. *Coord. Chem. Rev.* **2003**, *245*, 121–137.
- (20) The data from ref 11 were obtained in benzene solution on a different IR spectrometer and were not calibrated.
- (21) (a) Watanabe, T.; Oishi, S.; Fujii, N.; Ohno, H. *Org. Lett.* **2008**, *10*, 1759–1762. (b) Nakanishi, M.; Katayev, D.; Besnard, C.; Kundig, E. P. *Angew. Chem., Int. Ed.* **2011**, *50*, 7438–7441. (c) Anas, S.; Cordi, A.; Kagan, H. B. *Chem. Commun.* **2011**, 47, 11483–11485. (d) Katayev, D.; Nakanishi, M.; Bürgi, T.; Kündig, E. P. *Chem. Sci.* **2012**, *3*, 1422–1425. (e) Martin, N.; Pierre, C.; Davi, M.; Jassar, R.; Baudoin, O. *Chem. Eur. J.* **2012**, *18*, 4480. (f) Nakanishi, M.; Katayev, D.; Besnard, C.; Kündig, E. P. *Chimia* **2012**, *66*, 241–243.
- (22) Duisenberg, A. J. M.; Kroon-Batenburg, L. M. J.; Schreurs, A. M. M. *J. Appl. Crystallogr.* **2003**, *36*, 220–229.
- (23) Blessing, R. H. *Acta Crystallogr., Sect. A* **1995**, *51*, 33–38.
- (24) Sheldrick, G. M. *Acta Crystallogr., Sect. A* **2008**, *64*, 112–122.
- (25) Alcock, N. W.; Kemp, T. J.; Wimmer, F. L. *J. Chem. Soc., Dalton Trans.* **1981**, 635–638.